Journal of
Composites Science

MDPI

Article

Investigation of Thermomechanical and Dielectric Properties of PLA-CA 3D-Printed Biobased Materials

Morgan Lecoublet [1,2], Mohamed Ragoubi [1,*], Nathalie Leblanc [1] and Ahmed Koubaa [2]

[1] UniLaSalle, Unité de Recherche Transformations et Agro-Ressources (ULR 7519 UniLaSalle–Université d'Artois), 76130 Mont-Saint-Aignan, France; morgan.lecoublet@unilasalle.fr (M.L.); nathalie.leblanc@unilasalle.fr (N.L.)
[2] Laboratoire de Biomatériaux, Campus de Rouyn-Noranda, Université du Québec at Abitibi-Témiscamingue (UQAT), 445, Boul. de l'Université, Rouyn-Noranda, QC J9X 5E4, Canada; ahmed.koubaa@uqat.ca
* Correspondence: mohamed.ragoubi@unilasalle.fr; Tel.: +33-2-32-82-91-37

Abstract: Renewable dielectric materials have attracted the attention of industries and stakeholders, but such materials possess limited properties. This research focused on studying polylactic acid (PLA)/cellulose acetate (CA) blends produced by 3D printing to facilitate their integration into the electrical insulation field. The dielectric findings showed that a blend containing 40% of CA by weight had a dielectric constant of 2.9 and an electrical conductivity of 1.26×10^{-11} S·cm^{-1} at 100 Hz and 20 °C while exhibiting better mechanical rigidity in the rubbery state than neat PLA. In addition, it was possible to increase the electrical insulating effect by reducing the infill ratio at the cost of reduced mechanical properties. The differential scanning calorimetry, broadband dielectric spectroscopy, and dynamic mechanical analysis results showed that the PLA plasticizer reduced the energy required for PLA relaxations. These preliminary results demonstrated the benefits of using a combination of PLA, CA, and 3D printing for electrical insulation applications.

Keywords: biobased materials; 3D printing; dielectric properties; thermomechanical analysis

Citation: Lecoublet, M.; Ragoubi, M.; Leblanc, N.; Koubaa, A. Investigation of Thermomechanical and Dielectric Properties of PLA-CA 3D-Printed Biobased Materials. *J. Compos. Sci.* **2024**, *8*, 197. https://doi.org/10.3390/jcs8060197

Academic Editor: Francesco Tornabene

Received: 15 April 2024
Revised: 3 May 2024
Accepted: 21 May 2024
Published: 23 May 2024

1. Introduction

Dielectric materials are increasingly needed and produced for electronic applications in an increasingly connected world. The global electronic materials market has been estimated at USD 65.7 billion in 2022, with a 6% increase over the next 5 years [1]. This fast-paced production also raises issues such as the end of life of such materials. According to Ankit et al., 54 million tons of electronic waste have been produced in 2019, with a forecasted production of 75 million tons by 2030 [2]. Current e-waste management solutions are still inadequate, mainly based on landfill and incineration processes, with the associated pollution problems. Biobased materials would be highly desirable to mitigate such problems. These materials are more environmentally friendly than their synthetic counterparts in their manufacture, renewability, and biodegradability properties. According to the European Bioplastics association, 87 thousand tons of biobased materials were used in 2023 by the electronics industry, with an exponential increase predicted [3].

Two of the most well-known biobased polymers are polylactic acid and cellulose acetate. Nakatsuka produced plasticized PLA-coated electrical cables [4]. The plasticized PLA showed an electrical conductivity of 10^{-12} S·cm^{-1}, and the cable presented a dielectric strength (E_{BR}) of around 45 kV with good flexural properties while also showing insufficient plasticizer stability over time. By controlling the alignment of electrospun cellulose acetate (CA) fibers, Meng et al. controlled the CA/aluminum bimetal deformation [5]. These devices were used as actuators in a non-contact sensor for detecting the moisture content of a human hand, without showing any degradation in the electrical resistance of the aluminum part. This showed high potential in wearable health monitors and advanced

non-contact human–machine interactions. However, despite properties that make them attractive for use in electrical insulation applications as previously shown, these polymers face problems that limit their large-scale use, such as the drastic drop in the mechanical properties of PLA at temperatures above 60 °C [4], and the polar nature of CA [5]. One approach to mitigate such problems involves the use of polymer blending. In recent research, Coltelli et al. found that PLA/plasticized CA blends with a high PLA content gave heterogeneous blends with a pronounced tendency to form a fibrous-like morphology [6]. In addition, previous research carried out on PLA/plasticized CA showed that there was an interaction between the carbonyl groups of PLA and the hydroxyl groups of CA, greatly increasing the complex viscosity of the blends. In view of the applications of such blends in the dielectric field, Henning et al. proposed a PLA/CA blend filled with zinc pyrophosphate (ZnPP) as a biobased alternative to conventional printed circuit board (PCB) [7]. PLA/CA and PLA/CA blended with a ZnPP weight content (W_{ZnPP}) of 5% presented comparable dielectric properties to FR4 and FR2 glass/epoxy laminates, except for a significative lower dielectric constant and higher surface resistivity. They have been successfully used for PCB demonstrators, but issues remain unsolved, such as a warping effect during the soldering of components on its surface.

Three-dimensional printing is a promising technology in this sector as it allows extremely rapid and economical prototyping compared with conventional processes such as injection molding. The application of 3D printing for PLA/CA blends has been briefly studied for dielectric applications. Previously published results have demonstrated that such blends exhibited the results of dielectric and mechanical properties ranging between PLA and CA, offering design flexibility depending on the desired properties [4]. Furthermore, the 3D printing process can be used to directly tailor dielectric and mechanical properties by tuning the infill ratio [8]. Even if PLA/CA is a promising biobased polymeric for electronic applications, its application with the fused filament fabrication (FFF) technology is still largely undeveloped, and there is a lack of knowledge for electrical insulation applications. Their dielectric and thermomechanical performances should be optimized. To promote the use of biobased materials, this study proposes investigating the use of PLA/plasticized CA blends by 3D printing for electrical insulation applications to understand the advantages of such materials and their noted limitations.

2. Materials and Methods

2.1. Raw Materials

PLA-20003D (PLA) and ACI-002 plasticized cellulose acetate (CA) were supplied by respectively Natureplast (Caen, France) and EURL BBFil (Heiligenberg-Vallée, France). The possessed PLA presented a D-lactic acid content of 4.5%. The MFI given by suppliers for PLA and CA were, respectively, 6 g·10 min^{-1} (2.16 kg and 210 °C) and 15–30 g·10 min^{-1} (2.16 kg and 190 °C). The supplier gave the weight content of plasticizer into CA ($W_{plasticizer}$) at 29%.

2.2. Experimental Procedures

All materials were oven-dried for at least 4 h at 60 °C for all the processing steps to avoid internal moisture. A first extrusion processing was performed with a SCAMEX 25-20D (SCAMEX, Isques, France). A total of 5 conditions were produced, ranging from neat PLA to a PLA/CA blend containing 40% of CA by weight (named CA-40) and detailed in Table 1. A screw speed of 30 rpm and an extrusion profile temperature of 160-170-180 °C were used according to the preliminary tests.

The 3D filaments were produced with a 3DEVO filament maker (3DEVO, Utrecht, NLD) at the ITHEMM laboratory (Charleville-Mézières, France), with a screw speed of 5 rpm and an extrusion profile of 170-180-180-170 °C. The filament diameter was fixed at 2.85 mm as a compromise between diameter stability and filament quality. The 1.75 mm filaments manufactured were unsuitable for ensuring good printing quality.

Table 1. Produced conditions PLA/CA blends (W_{PLA} correspond to PLA content by weight and W_{CA} correspond to CA content by weight).

	PLA	CA-10	CA-20	CA-30	CA-40
WPLA (%)	100	90	80	70	60
WCA (%)	0	10	20	30	40

The fused filament fabrication (FFF) was performed with a SIGMAX R19 3D printing device (BCN3D, Gavà, SPA). The parameters used were resumed in Table 2, and the produced samples were presented in Figure 1. Printing problems have been noted when the filaments were not stored in desiccators, so during the entire printing stage, the filaments were stored in desiccators. All samples achieved good quality without warping or cracking. A glue stick had to be applied to the glass bed to increase adhesion only for CA-30 and CA-40 conditions. Before their characterization, all samples were stored in a desiccator for 3 h.

Table 2. Three-dimensional parameters conditions.

Nozzle temperature	215 °C
Nozzle size	0.8 mm
Printing speed	30 mm·s^{-1}
Sample thickness	2 and 4 mm
Layer thickness	0.2 mm
Infill pattern (BDS)	Concentric
Infill pattern (DMA)	±45
Bed temperature	60 °C

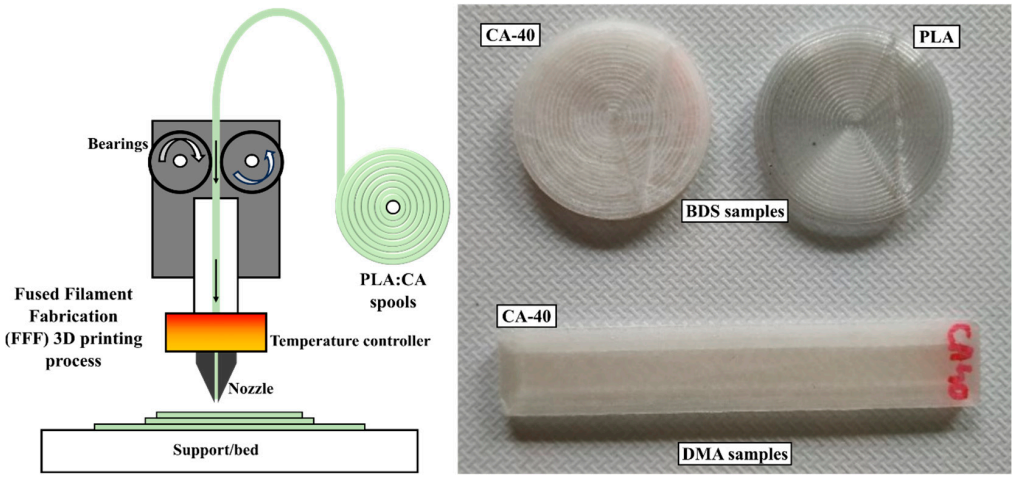

Figure 1. Fused filament fabrication (FFF) 3D printing process and produced samples.

2.3. Characterization Methods

All the figures presented below were produced using the Python 3.10.11 programming language and the Pandas' module to read the dataset and Matplotlib to produce the different graphs.

2.3.1. Differential Scanning Calorimetry (DSC) Analysis

Differential scanning calorimeter (DSC) analyses were proposed to observe the thermal properties and the crystallinity of the materials. The measurements were performed on a DSC 214 Polyma (Netzsch, Selb, Germany) with 15 mg of material, inserted in Al pans. The used protocol consisted of one heating and one cooling ramp between 20 and 180 °C with a heating rate of 10 K·min^{-1} and an argon flow of 20 mL·min^{-1}. The crystallinity content (X_{cr}) were determined according to Equation (1) developed for PLA/CA blends [9]:

$$X_{cr} = \frac{dH}{dH_0 * (W_{cr})} * 100 \quad (1)$$

where dH is the measured crystallization enthalpy, dH_0 is the melting enthalpy of the theoretical 100% crystalline polymer 100%, both expressed in $J \cdot g^{-1}$. W_{PLA} is the weight percentage of PLA.

2.3.2. Dynamic Mechanical Analysis (DMA)

DMA was carried out on 60 × 10 × 2 mm and 60 × 10 × 4 mm samples with an Artemis DMA 242 E (Netschz, Selb, Germany). The double cantilever method was chosen over the 3-point bending method due to the very low stiffness of PLA once its glass transition temperature is reached (T > 60 °C). The protocol consisted of a ramp between 30 and 140 °C at 5 °C·min^{-1}. The controlled force has been set at 1 Hz, which is the frequency usually used in the literature.

2.3.3. Broadband Dielectric Spectroscopy (BDS) Analysis

BDS tests were carried out using a Keysight E4980A Precision LCR Meter (Agilent Technologies, Santa Rosa, CA, USA) on 25 mm disk samples. The heating program consisted of an isothermal rise between 0 and 160 °C with 4 °C per step and measured at 100 Hz. The dielectric constant ε' is expressed according to Equation (2) [10]:

$$\varepsilon' = \frac{C_p * ep}{\varepsilon_0 * S} \quad (2)$$

where C_p is the electrical capacitance given in Farad, S is the cross-sectional area of the sample (in m^2), ep is the distance between electrodes (in m), and ε_0 is the vacuum permittivity (given as 8.541878 × 10^{-12} F·m^{-1}). The electrical conductivity σ_{AC} can be determined with Equation (3) [10]:

$$\sigma_{ac} = \omega * \varepsilon'' * \varepsilon_0 = 2\pi f * \varepsilon'' * \varepsilon_0 \quad (3)$$

where σ_{AC} is expressed in S·m^{-1}, ω is the angular frequency, and f is the applied electrical frequency (in Hz).

3. Results

Figure 2 presents the thermal properties of neat PLA and PLA/CA blends. Neat PLA exhibited all the expected relaxations for a PLA: a glass temperature (T_g) of 61.6 °C, a cold crystallization temperature (T_{cc}) of 126.8 °C, and a melting temperature (T_m) of 156.3 °C [11]. Adding CA decreased all the observed relaxations. At W_{CA} = 40%, the T_g, T_{cc}, and T_m of PLA decreased by 21.3, 23.9, and 8.5 °C, respectively. Kang et al. have also observed a decrease in T_g by adding plasticizers into PLA [11]. According to the latter, adding plasticizers, generally small molecules, increased the free volume of macromolecular chains, thereby improving the polymer's mobility. It is also worth noting that the supplied PLA was amorphous, with a measured X_{cr} below 1%. Furthermore, while adding the plasticizer improved the mobility of the macromolecular chains, it did not significantly change the crystallinity of the blends, with X_{cr} still below 1%. The only visible change is the presence of a second slight melting peak at around 142 °C, proof that a second crystal lattice appeared.

As the DSC findings demonstrated, the addition of CA altered the thermal properties of PLA by lowering the relaxation energies. Dielectric materials were subjected to various temperature fluctuations due to electric current, which could affect their dielectric properties. An understanding of the thermal dielectric stability would be important to qualify the presented materials. Figure 3 presents the dielectric constant (ε') and electrical conductivity (σ_{AC}) of the 3D-printed neat PLA and CA-40 with an infill ratio of 100% versus temperature. At 20 °C, PLA and CA-40 presented a ε' of 2.53 and 2.81, respectively, and a σ_{AC} of 4.8 × 10^{-13} and 1.4 × 10^{-12} S·cm^{-1}, respectively. We thought that the increase in dielectric properties was attributed to the polar nature of CA, which could contain more

hydroxyl functions than PLA [5]. Although the addition of CA increased the electrical conductivity of the blends, the measured properties at 100 Hz for all materials were still in the electrically insulating range [12], validating their use for dielectric applications. However, the produced materials showed notable temperature sensitivity. At 160 °C, PLA exhibited a ε' and σ_{AC} of 1.92 and 503 times greater, respectively, and CA-40 exhibited a ε' and σ_{AC} of 1.85 and 145 times greater, respectively, than measured at 20 °C. The observations for neat PLA are in perfect agreement with the literature [5,13]. Badia et al. have also noticed that measured at 100 Hz, the dielectric constant of neat PLA increased from 3.05 to 3.95 when the temperature shifted from 20 to 130 °C [13]. The temperature-dependent behavior observed in both electrical conductivity and dielectric constant can be associated with the increased ionic mobility of macromolecular chains, as mentioned in the literature [5]. As the melting temperature approached, the σ_{AC} increased faster for CA-40 than neat PLA. This could also be due to the increased free volume, greatly improving the mobility of the carrier charges [14]. CA reduced the energy required for α-relaxation measured by BDS, as observed in the literature when a plasticizer is added to a plastic matrix. CA-40 showed an α-relaxation shift of −20 °C. While ε' and σ_{AC} were slightly higher for CA-40 than for PLA in the measurement range tested, these results remained comparable and low enough to be suitable for electrical insulation applications.

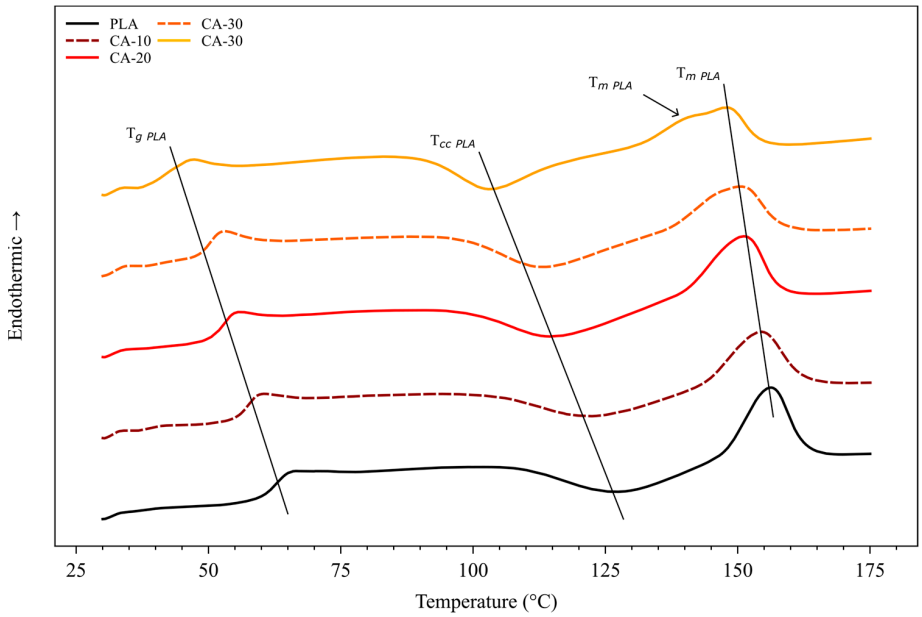

Figure 2. DSC thermograms of PLA/CA blends.

As the field of dielectric materials covers applications requiring high flexibility or high rigidity, it is also important to know the thermomechanical behavior of the proposed materials. PLA suffers from an important loss of mechanical properties beyond its T_g due to its rubbery state. As the incorporation of plasticized CA into PLA will result in a complex behavior, it is important to understand its behavior [5]. Figure 4 presents the storage modulus (E′) and loss factor (tan δ) of the 3D-printed neat PLA and CA-40 with an infill ratio of 100% versus temperature. PLA also presented a typical amorphous behavior. A rigid glassy behavior is noted at T < 60 °C, with an E′ value of 1.81 GPa at 30 °C. Once reaching the T_g, the storage modulus sharply decreased, reaching its lowest value at around 96 °C. At this temperature, the E′ reached 4.0 MPa, i.e., a reduction of 450 times in stiffness between 30 and 96 °C. Once the minimum has been reached, the mechanical rigidity increased due to the formation of the crystal lattice resulting from the cold crystallization of PLA. The addition of CA slightly reduced the E′ of PLA, with an E′ of 1.69 GPa obtained for CA-40, i.e., a mechanical rigidity reduction of 7%. At 30 °C, PLA and CA-40 showed an E′ of 1.81 and 1.69 GPa, respectively. Although the addition of CA in the glassy state decreased

the E′ and increased the tan δ, the CA addition appeared attractive from a mechanical point of view, as it seems to greatly limit the loss of mechanical properties when PLA reached the rubbery state. This improvement effect can be directly linked to the CA and not to an improvement in the blend's crystallinity, as demonstrated by DSC. Moreover, the tan δ was much lower in the rubbery state, so less electromagnetic energy was converted into heat. It is also worth noting that for both DMA and BDS measurements, the addition of CA decreased the α-relaxation and cold crystallization temperature of PLA, in agreement with DSC analysis.

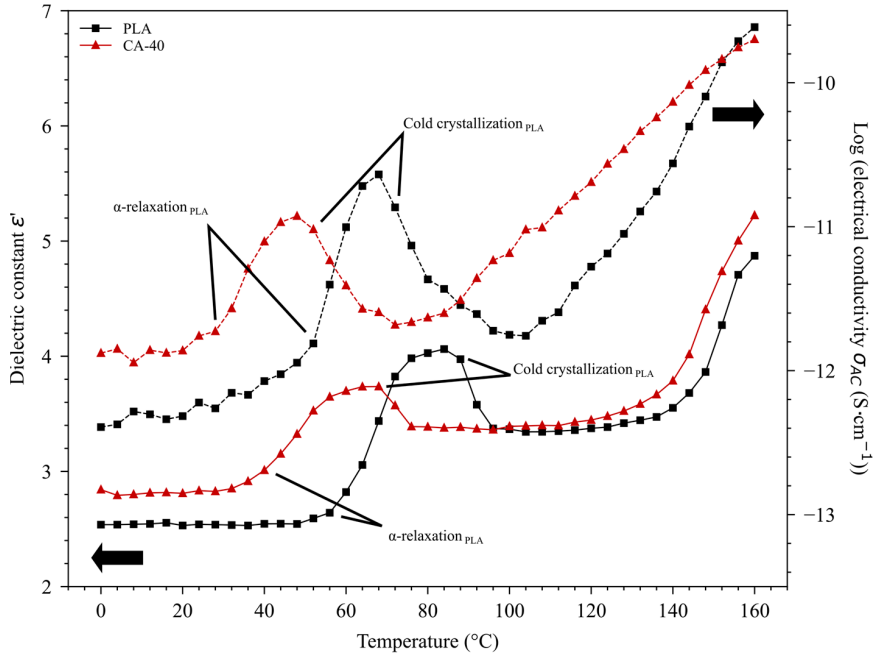

Figure 3. Dielectric constant ε′ and electrical conductivity σ_{AC} of PLA and CA-40 versus temperature, measured at 100 Hz. The main arrows indicate the axes of the corresponding curves.

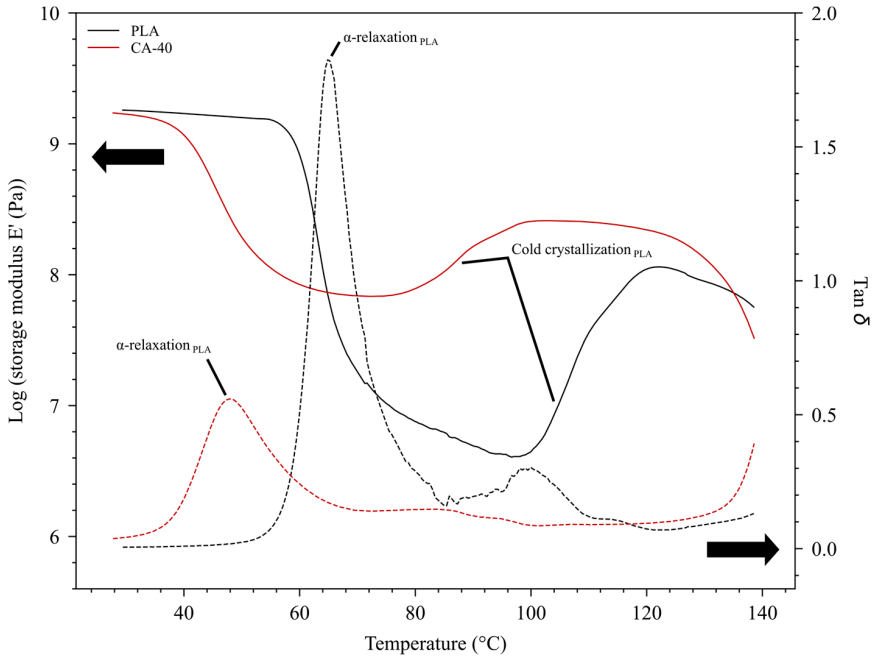

Figure 4. Log (storage modulus E′) and loss tangent tan δ of PLA and CA-40 specimens versus temperature. The main arrows indicate the axes of the corresponding curves.

One of the main benefits of 3D printing is the ability to control the infill ratio of 3D specimens. Zhang et al. demonstrated that the dielectric constant was proportionally related to the infill ratio, which can be valuable for producing materials with controlled dielectric properties [15]. To investigate this effect on the mechanical and dielectric properties of PLA/CA blends, Figure 5 shows the ε', σ_{AC}, and E′ of CA-20, CA-30, and CA-40 blends. The ε' and E′ decreased with a decreasing infill ratio, while the σ_{AC} increased with decreasing infill ratio. In the case of CA-40, shifting from 100% to 40%, the infill ratio decreased the dielectric constant and storage modulus by 29% and 61%, respectively. The σ_{AC} was, however, increased by 216%. The decrease in ε' and E′ with a decreasing infill ratio can be directly related to the porosity rate of the samples [15–17]. Regarding the variation in the dielectric constant with the infill ratio, two studies in the literature can provide information on the involved mechanism. Figure 6 shows the ε' versus infill ratio of the work by Zhang et al. and Colella et al., using 3D-printed PLA [15,18]. It can be noted that the theoretical model was linear for both studies. Lowering the infill ratio logically produced less dense samples that were, therefore, less likely to be polarized, as the dielectric constant of air approaches 1 [8]. It is worth noting that linear regression applied to literature data gives a value very close to 1, validating this statement. The increase in the electrical insulating properties associated with the reduction in the infill ratio can be linked to more conductive paths, enabling the electrical current to bypass areas of high local resistance due to greater local heterogeneity. These results demonstrate that improving the insulating properties of PLA/CA blends would be possible by reducing the infill ratio at the cost of lower mechanical stiffness.

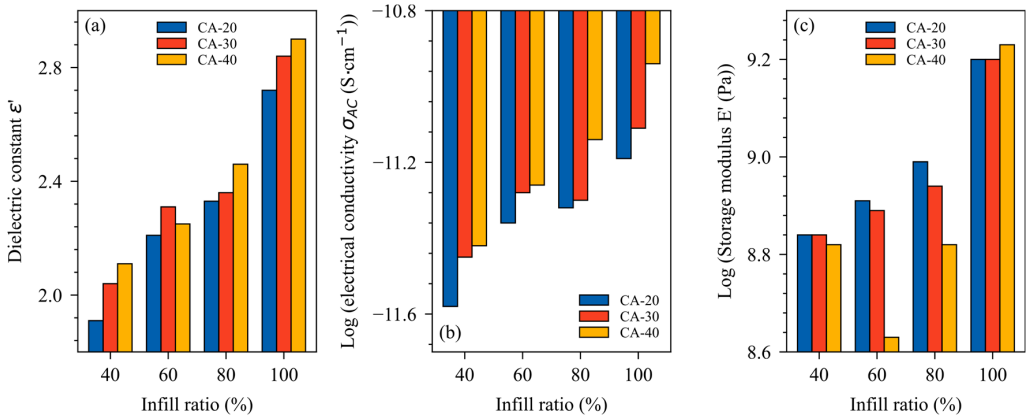

Figure 5. (**a**) Dielectric constant ε', (**b**) electrical conductivity σ_{AC} and (**c**) log (storage modulus E′) as a function of infill ratio measured on 4 mm thick samples. Dielectric constant and electrical conductivity are measured at 100 Hz and 20 °C, and storage modulus is measured at 30 °C and 1 Hz.

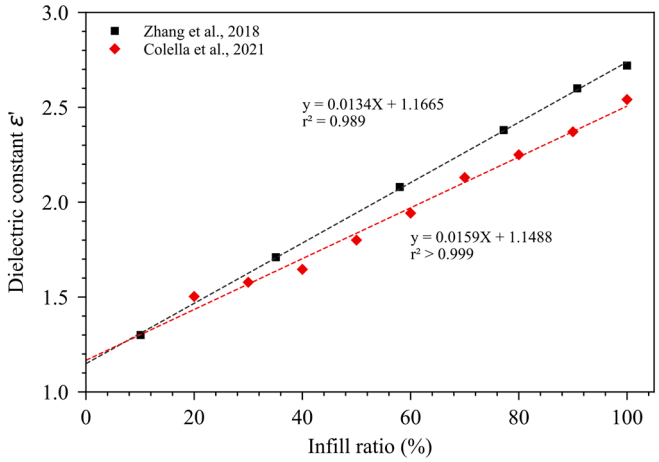

Figure 6. Dielectric constant ε' versus infill ratio of 3D-printed PLA [15,18].

To compare these new materials with their synthetic counterparts, Table 3 presents a comparative analysis of the tested properties of CA-40 and LDPE as reported in the literature. These results show that CA-40 with 40% infill had a storage modulus and electrical conductivity equivalent to LDPE, with a lower dielectric constant than LDPE. This would prove that the 3D printing of PLA/CA blends is relevant to replace dielectric applications usually dominated by LDPE, such as electrical insulation, cable insulation, and antistatic and electromagnetic shielding.

Table 3. Comparative analysis of the tested properties of CA-40 and LDPE as reported in the literature.

	Dielectric Constant ε'			Electrical Conductivity σ_{AC} ($S \cdot cm^{-1}$)			Storage Modulus E' (MPa)		
Material	**T (°C)**	**Value**	**Ref**	**T (°C)**	**Value**	**Ref**	**T (°C)**	**Value**	**Ref**
CA-40	20	2.11	Our study	20	4×10^{-12}	Our study	30	656	Our study
LDPE	Room T	2.43	[19]	20	3×10^{-13}	[20]	30	380	[21]
LDPE	Room T	2.21	[22]	27	3×10^{-12}	[23]	30	230	[24]
LDPE	Room T	2.46	[25]	30	1×10^{-12}	[26]	30	205	[24]

4. Conclusions

In this study, we investigated the dielectric and thermomechanical properties of 3D-printed PLA/CA blends to determine the benefits and limitations of such materials for electrical insulation applications. The CA content and infill ratio were the main criteria in the dielectric and mechanical response of PLA/CA blends. We highlighted that adding CA improved the thermomechanical stability of PLA in the rubbery state. Moreover, electric insulation performances were improved by reducing the infill ratio of the 3D-printed samples. Under the chosen conditions, the infill ratio had a greater effect on the mechanical and dielectric properties than the effect of CA, showing that adjusting the dielectric properties of PLA/CA blends by adjusting these crucial parameters is possible. Our results show that these PLA/CA blends are promising for insulation electrical applications, at the cost of a decrease in mechanical properties in the glassy state and a slight decrease in electrical insulating properties. To go further, it would be possible to analyze in depth the influence of post-crystallization on the mechanical stability. Furthermore, to limit the plasticizing effect of CA, we can reduce the plasticizer content to fully benefit from the insulating effect of PLA and the improved mechanical stability at high temperatures provided by CA. This research also opens the way to numerous research opportunities. Investigations could be pursued by introducing micro or nanosized biobased fillers to increase thermomechanical stability at high temperature. In addition, 3D printing can be exploited for the creation of functional gradient structures, as well as customized design for specific dielectric applications, such as high-voltage insulation and antistatic and electromagnetic shielding.

Author Contributions: M.L.: Conceptualization, Methodology, Investigation, Software, Data curation, Roles/Writing—original draft. M.R.: Conceptualization, Supervision, Roles/Writing—original draft, review and editing. N.L.: Supervision, review and editing. A.K.: Conceptualization, Supervision, Writing—review and editing. All authors have read and agreed to the published version of the manuscript.

Funding: This research was funded by MITACS Globalink Program, Normandy region and TABES Create Program (Grant Number CREATE 554777-2021).

Data Availability Statement: The data presented in this study are available on request from the corresponding author.

Acknowledgments: Authors acknowledge financial support from NSERC, Canada Research Chair program, MITACS Globalink Program; Normandy region, research fellowship grant; and AGRO-BIOTECH platform from UniLaSalle-Rouen for the great help for dielectric measurements.

Conflicts of Interest: The authors declare no conflicts of interest.

References

1. TechSci Research. *Electronic Materials Market Size and Trends 2028*; TechSci Research: Noida, India, 2023.
2. Ankit; Saha, L.; Kumar, V.; Tiwari, J.; Sweta; Rawat, S.; Singh, J.; Bauddh, K. Electronic Waste and Their Leachates Impact on Human Health and Environment: Global Ecological Threat and Management. *Environ. Technol. Innov.* **2021**, *24*, 102049. [CrossRef]
3. *European Bioplastic Applications/Sectors*; European Bioplastics e.V.: Berlin, Germany, 2023.
4. Lecoublet, M.; Ragoubi, M.; Leblanc, N.; Koubaa, A. Dielectric and Viscoelastic Properties of 3D-Printed Biobased Materials. *Ind. Crops Prod.* **2024**, *212*, 118354. [CrossRef]
5. Lecoublet, M.; Ragoubi, M.; Leblanc, N.; Koubaa, A. Dielectric and Rheological Performances of Cellulose Acetate, Polylactic Acid and Polyhydroxybutyrate-Co-Valerate Biobased Blends. *Polymer* **2023**, *285*, 126358. [CrossRef]
6. Henning, C.; Schmid, A.; Hecht, S.; Ruckmar, C.; Harre, K.; Bauer, R. Usability of Bio-Based Polymers for PCB. In Proceedings of the 2019 42nd International Spring Seminar on Electronics Technology (ISSE), Wroclaw, Poland, 15–19 May 2019; IEEE: Piscataway, NJ, USA, 2019; pp. 1–7.
7. Lecoublet, M.; Ragoubi, M.; Kenfack, L.B.; Leblanc, N.; Koubaa, A. How Do 3D Printing Parameters Affect the Dielectric and Mechanical Performance of Polylactic Acid–Cellulose Acetate Polymer Blends? *J. Compos. Sci.* **2023**, *7*, 492. [CrossRef]
8. El Assimi, T.; Blažic, R.; Vidović, E.; Raihane, M.; El Meziane, A.; Baouab, M.H.V.; Khouloud, M.; Beniazza, R.; Kricheldorf, H.; Lahcini, M. Polylactide/Cellulose Acetate Biocomposites as Potential Coating Membranes for Controlled and Slow Nutrients Release from Water-Soluble Fertilizers. *Prog. Org. Coat.* **2021**, *156*, 106255. [CrossRef]
9. Benabed, F.; Seghier, T. Dielectric Properties and Relaxation Behavior of High Density Polyethylene (HDPE). *Appl. Mech. Mater.* **2015**, *799–800*, 1319–1324. [CrossRef]
10. Jacob, M.; Varughese, K.T.; Thomas, S. Dielectric Characteristics of Sisal–Oil Palm Hybrid Biofibre Reinforced Natural Rubber Biocomposites. *J. Mater. Sci.* **2006**, *41*, 5538–5547. [CrossRef]
11. Chaochanchaikul, K.; Pongmuksuwan, P. Influence of Ozonized Soybean Oil as a Biobased Plasticizer on the Toughness of Polylactic Acid. *J. Polym. Environ.* **2022**, *30*, 1095–1105. [CrossRef]
12. Solazzo, M.; O'Brien, F.J.; Nicolosi, V.; Monaghan, M.G. The Rationale and Emergence of Electroconductive Biomaterial Scaffolds in Cardiac Tissue Engineering. *APL Bioeng.* **2019**, *3*, 041501. [CrossRef] [PubMed]
13. Badia, J.D.; Reig-Rodrigo, P.; Teruel-Juanes, R.; Kittikorn, T.; Strömberg, E.; Ek, M.; Karlsson, S.; Ribes-Greus, A. Effect of Sisal and Hydrothermal Ageing on the Dielectric Behaviour of Polylactide/Sisal Biocomposites. *Compos. Sci. Technol.* **2017**, *149*, 1–10. [CrossRef]
14. Bandara, T.M.W.J.; Dissanayake, M.A.K.L.; Albinsson, I.; Mellander, B.-E. Mobile Charge Carrier Concentration and Mobility of a Polymer Electrolyte Containing PEO and Pr4N+I− Using Electrical and Dielectric Measurements. *Solid State Ion.* **2011**, *189*, 63–68. [CrossRef]
15. Zhang, S.; Arya, R.K.; Pandey, S.; Vardaxoglou, Y.; Whittow, W.; Mittra, R. 3D-Printed Planar Graded Index Lenses. *IET Microw. Antennas Propag.* **2016**, *10*, 1411–1419. [CrossRef]
16. Kuzmanić, I.; Vujović, I.; Petković, M.; Šoda, J. Influence of 3D Printing Properties on Relative Dielectric Constant in PLA and ABS Materials. *Prog. Addit. Manuf.* **2023**, *8*, 703–710. [CrossRef] [PubMed]
17. Öteyaka, M.Ö.; Aybar, K.; Öteyaka, H.C. Effect of Infill Ratio on the Tensile and Flexural Properties of Unreinforced and Carbon Fiber-Reinforced Polylactic Acid Manufactured by Fused Deposition Modeling. *J. Mater. Eng. Perform.* **2021**, *30*, 5203–5215. [CrossRef]
18. Colella, R.; Chietera, F.P.; Catarinucci, L. Analysis of FDM and DLP 3D-Printing Technologies to Prototype Electromagnetic Devices for RFID Applications. *Sensors* **2021**, *21*, 897. [CrossRef] [PubMed]
19. Ahmed Dabbak, S.; Illias, H.; Ang, B.; Abdul Latiff, N.; Makmud, M. Electrical Properties of Polyethylene/Polypropylene Compounds for High-Voltage Insulation. *Energies* **2018**, *11*, 1448. [CrossRef]
20. Noorunnisa Khanam, P.; Al-Maadeed, M.A.; Mrlik, M. Improved Flexible, Controlled Dielectric Constant Material from Recycled LDPE Polymer Composites. *J. Mater. Sci. Mater. Electron.* **2016**, *27*, 8848–8855. [CrossRef]
21. Chen, J.-Q.; Wang, X.; Sun, W.-F.; Zhao, H. Improved Water-Tree Resistances of SEBS/PP Semi-Crystalline Composites under Crystallization Modifications. *Molecules* **2020**, *25*, 3669. [CrossRef] [PubMed]
22. Han, B.; Yin, C.; Chang, J.; Pang, Y.; Lv, P.; Song, W.; Wang, X. Study on the Structure and Dielectric Properties of Zeolite/LDPE Nanocomposite under Thermal Aging. *Polymers* **2020**, *12*, 2108. [CrossRef] [PubMed]
23. Ciuprina, F.; Plesa, I. DC and AC Conductivity of LDPE Nanocomposites. In Proceedings of the 2011 7th International Symposium on Advanced Topics in Electrical Engineering (ATEE), Bucharest, Romania, 12–14 May 2011; pp. 1–6.
24. Poh, L.; Wu, Q.; Chen, Y.; Narimissa, E. Characterization of Industrial Low-Density Polyethylene: A Thermal, Dynamic Mechanical, and Rheological Investigation. *Rheol. Acta* **2022**, *61*, 701–720. [CrossRef]
25. Kemari, Y.; Teyssedre, G.; Mekhaldi, A.; Teguar, M. Dielectric Properties and Beta-Relaxation in Cross- Linked Polyethylene: Effect of Thermal Aging. In Proceedings of the 2020 IEEE 3rd International Conference on Dielectrics (ICD), Valencia, Spain, 5–31 July 2020; IEEE: Piscataway, NJ, USA, 2020; pp. 73–76.
26. Stancu, C.; Notingher, P.V.; Panaitescu, D.; Marinescu, V. Electrical Conductivity of Polyethylene-Neodymium Composites. In Proceedings of the 2013 8th International Symposium on Advanced Topics in Electrical Engineering (ATEE), Bucharest, Romania, 23–25 May 2013; IEEE: Piscataway, NJ, USA, 2013; pp. 1–6.